Peiming Zheng, Sachie Yagami, Dan Aoki*, Masato Yoshida, Yuzou Sano*, Yasuyuki Matsushita and Kazuhiko Fukushima

The composition and chemical alteration of gums in the vessels of *Phellodendron amurense*

https://doi.org/10.1515/hf-2017-0057
Received April 11, 2017; accepted July 14, 2017; previously published online August 14, 2017

Abstract: An occluding substance (gum) was observed in the vessels of *Phellodendron amurense* Rupr. and analysed by spectroscopic and chemical methods. Following safranin-alcian blue staining, the gum in sapwood (sW) turned to blue and in heartwood (hW) to red. The gum was studied *in situ* by UV and Raman microscopies, time-of-flight secondary ion mass spectrometry (TOF-SIMS). The gum was isolated by laser microdissection (LMD) and it was alkali hydrolysed and the degradation products were analysed by GC-MS. The staining experiments, and the UV and Raman microscopies indicated that the major component of the sW gum is constituted of polysaccharides, while in the hW gum the aromatic character is dominating. TOF-SIMS measurements were interpreted as showing the aromatic substances in the hW gum did not contain lignin. The GC-MS analysis revealed the presence of vanillic acid in the degradation products of hW gum.

Keywords: gum, heartwood, laser microdissection, *Phellodendron amurense*, Raman microscopy, sapwood

Introduction

In vessel-bearing angiosperm trees, vessels are frequently occluded by outgrowths that originate from the adjacent axial and/or ray parenchyma cells after the vessels become dysfunctional (Zimmerman 1983; Hillis 1987; Evert 2006). The vessel occlusions in trees are usually tyloses and gums, the type of which largely depends upon the size of the vessel-parenchyma pits (Chattaway 1949; Bonsen and Kučera 1990; Saitoh et al. 1993; Fujii et al. 2001). Vessel occlusions have often been described in relation to heartwood (hW) formation, injuries or infection of pathogens, but on the other hand, there is some empirical evidence that the occlusions are formed as a response to air embolisms in the vessels (Zimmerman 1983; Hillis 1987; Rioux et al. 1998; De Micco et al. 2016). Indeed, all types of vessel occlusions can be found in normal sapwood (sW) across many species (Bonsen and Kučera 1990; Rioux et al. 1998; Wheeler 2011; De Micco et al. 2016).

Tyloses generally consist of primary and secondary walls as it is the case in normal cells, and consist of cellulose, hemicelluloses and lignin (Foster 1967; Pearce and Holloway 1984; Barnett et al. 1993; De Micco et al. 2016). Gums are generally colourless, nontoxic, odourless and usually tasteless. On desiccation or exposure to air, they become to hard, clear and glassy masses (Hillis 1987). Little is known regarding the chemical components of gums that occlude vessels. Studies on the composition and chemical alteration of gums are very important for a better understanding not only in terms of the mechanism of gum formation but also from the points of view of biological properties of the living trees, tree physiology and wood technology (Saitoh et al. 1993; Rioux et al. 1998; De Micco et al. 2016).

Gums were studied by histochemical staining techniques. Gagnon (1967) concluded that gums in *Ulmus americana* comprise lignin and pectin, which was deduced from positive staining reactions. Rioux et al. (1998) reported that pectin appears to be the basic component of gums, while phenols and polysaccharides were also detected either as an integral part of the occlusions, or as accumulations alongside them in the vessels. However, histochemical stains are not very specific as they may react with various constituents of the plant tissues (Rioux et al. 1998). Fujita et al. (1977) collected a gum-like substance from sW blocks of *Albizia julibrissin* that had been incubated by the method of Meyer (1967), and demonstrated

***Corresponding authors: Dan Aoki,** Graduate School of Bioagricultural Sciences, Nagoya University, Chikusa-ku, Nagoya 464-8601, Japan, Phone: +81-52-789-4062, Fax: +81-52-789-4163, e-mail: daoki@agr.nagoya-u.ac.jp; and **Yuzou Sano,** Research Faculty of Agriculture, Hokkaido University, Sapporo 060-8589, Japan, Phone: +81-11-706-2516, Fax: +81-11-706-3859, e-mail: pirika@for.agr.hokudai.ac.jp
Peiming Zheng: School of Life Science, Shandong University, Jinan, China; and Graduate School of Bioagricultural Sciences, Nagoya University, Nagoya, Japan
Sachie Yagami, Masato Yoshida, Yasuyuki Matsushita and Kazuhiko Fukushima: Graduate School of Bioagricultural Sciences, Nagoya University, Nagoya, Japan

Brought to you by | Nagoya University
Authenticated
Download Date | 1/29/18 5:53 AM

by IR spectroscopy and gas chromatography that the substance is constituted of polysaccharides, while mannose and galactose were detected as degradation products. The differences in native gum composition in sW and hW have not yet been investigated.

To investigate the chemical composition of specific tissues in plants such as gums, special instruments are needed with high local resolution such as Raman microscopy (Fischer et al. 2005; Peetla et al. 2006; Schenzel et al. 2009; Gierlinger et al. 2010). Time-of-flight secondary ion mass spectrometry (TOF-SIMS) is a high resolution instrument which provides mass spectral information at the submicron resolution level (Lee et al. 2012; Zheng et al. 2014a, 2016, 2017; Aoki et al. 2016a,b). On the other hand, laser microdissection (LMD) is an established tool employed in wood research for the collection of specific tissues under direct microscopic observation (Nakazono et al. 2003; Zheng et al. 2014b, 2016).

The gums occurring in vessels of *Phellodendron amurense* Rupr. were the focus of the present study. The wood is ring-porous, and gums are commonly present in the wide vessels located in the earlywood in both sW and hW (Saitoh et al. 1993). The analytical tools listed above, i.e. Raman microscopy and TOF-SIMS in combination with UV microscopy and staining experiments, will be applied for the characterisation of sW and hW gums. Gum samples will also be collected by the LMD technique, and the isolated material will be degraded by alkaline hydrolysis and the resulting product will be detected by GC-MS.

Materials and methods

Materials: Herbarium specimens (disks of 50-mm thickness) were collected on October 2004 from the main trunk of *P. amurense* Rupr., which grows in the natural forests of the Tomakomai Experimental Forest, Hokkaido University, Japan. The stems contained 38 annual rings and a diameter of 150 mm at breast height. Annual rings nos. 1–4 were distinguished as sW and the rings nos. 5–38 as hW based on colour differences. Blocks ($10\times10\times10$ mm^3) containing continuous annual rings nos. 1–9 were studied.

Histochemical staining: The blocks were immersed in water for more than 7 days. Then, 15-µm-thick transverse sections were sliced by a sliding microtome (LS-113, Yamato Kohki Industrial Co., Ltd., Saitama, Japan). Parts of the sections were extracted with NaOHaq (1 M, 60°C, 4 h), HClaq (1 M, 60°C, 4 h), MeOH (r.t., 7 days) and DMSO (r.t., 7 days), respectively. The intact and treated sections mentioned above were double-stained with 1% safranin-alcian blue (Scott and Dorling 1965; Nassar et al. 2008; Harem and Liman 2009) and permanent slides were prepared. Finally, the stained sections were examined under an optical microscope (BX50, Olympus Corp., Tokyo, Japan).

UV microscopy: The transverse sections (1-µm thickness) from the sW and hW were prepared from the samples embedded in Quetol 812 epoxy resin using a diamond knife on an ultra-microtome (HM350, Microm). The sections were photographed at 280 nm (MPM800, Carl Zeiss).

Raman microscopy: The transverse sections (100-µm thickness) containing sW and hW were submitted to Raman microscopy analysis (LabRam HR Evolution, Horiba Jobin Yvon, Kyoto, Japan). The micro cuts were immersed in H_2O to reduce the intrinsic fluorescence. Measurement conditions: acquisition time 1 s (60×); laser wavelength 633 nm; hole diameter 80 µm; slit width 100 µm; magnification 60×. The gums in annual ring nos. 3 and 8 were considered as sW and hW gums, respectively. The measurement was replicated with different gums in the same annual ring.

TOF-SIMS: The transverse sections (100-µm thickness) containing sW and hW were submitted for TOF-SIMS analysis (TRIFT III, ULVAC-PHI, Chigasaki, Japan). Positive ion spectra of gums in sW and hW were collected. Measurement conditions: primary ion 22 keV Au_1^+; pulse width of 1.8 ns for bunched spectrum mode; mass range, m/z 0.5–1850. A low-energy pulsed electron gun (30 eV) was used for the surface charge compensation. All TOF-SIMS data were obtained as "raw" data files, recording a full mass spectrum at every 256×256 pixel points. The gum specific spectra were obtained via the region-of-interest (ROI) function of WinCadence 5.1.2.8 (ULVAC-PHI, Inc.). The measurement was conducted for 10 individual gums in both the sW and hW regions.

LMD collection of gums: LMD collection was operated according to Zheng et al. (2014b, 2016). The dry sections from the sW (Figure 1a) and hW (Figure 1c) were fixed with adhesive tape covering a hole (12 mm in diameter) in a plastic plate and then dissected under microscopic observations (LMD7000, Leica Microsystems, Tokyo, Japan). Fragments enriched with gums from the sW and hW were individually collected in sample tubes (Figure 1b and d). The molecules at the cutting edge of the cut fragments are damaged to a certain degree by the laser (Nakashima et al. 2008; Zheng et al. 2014b, 2016). This is the reason why laser targeting lines were drawn in the region of the neighbouring axial elements to minimise the gums damage.

Chemical analysis: The LMD-collected 0.5-mg gums (ca. 1500 fragments) from the sW and hW were treated with 0.5 ml NaOHaq (1 M) at 60°C for 24 h. The pH of the reaction solution was then adjusted to ca. 2–3 and extracted by ethyl acetate (3×5 ml). The supernatant liquid was concentrated to about 1.5 ml and stored at 4°C. The residues were dried at room temperature and treated with 0.5 ml NaOHaq (2 M) at 170°C for 2 h. Then the pH of the reaction solution was adjusted to ca. 2–3 and extracted by ethyl acetate (3×5 ml). The supernatant liquid was concentrated to about 1.5 ml and stored at 4°C. The intact wood sections (not treated by LMD) of the sW and hW were also hydrolysed by NaOHaq (1 M and 2 M) as described above. The intact wood sections contained trace amounts of the gums though this should be negligible. All analyses were performed in triplicates.

The alkaline hydrolysate was analysed by GC-MS (QP 2010, Shimadzu, Kyoto, Japan) equipped with a capillary column (Rxi – 1m, 30 m × 0.32 mm, film thickness of 0.25 µm). GC-MS conditions: injector 250°C; temperature program 100°C (1 min), 100→280°C (5°C min^{-1}), and 280°C (10 min); carrier gas He; flow rate 1.6 ml min^{-1}; interface

Brought to you by | Nagoya University
Authenticated
Download Date | 1/29/18 5:53 AM

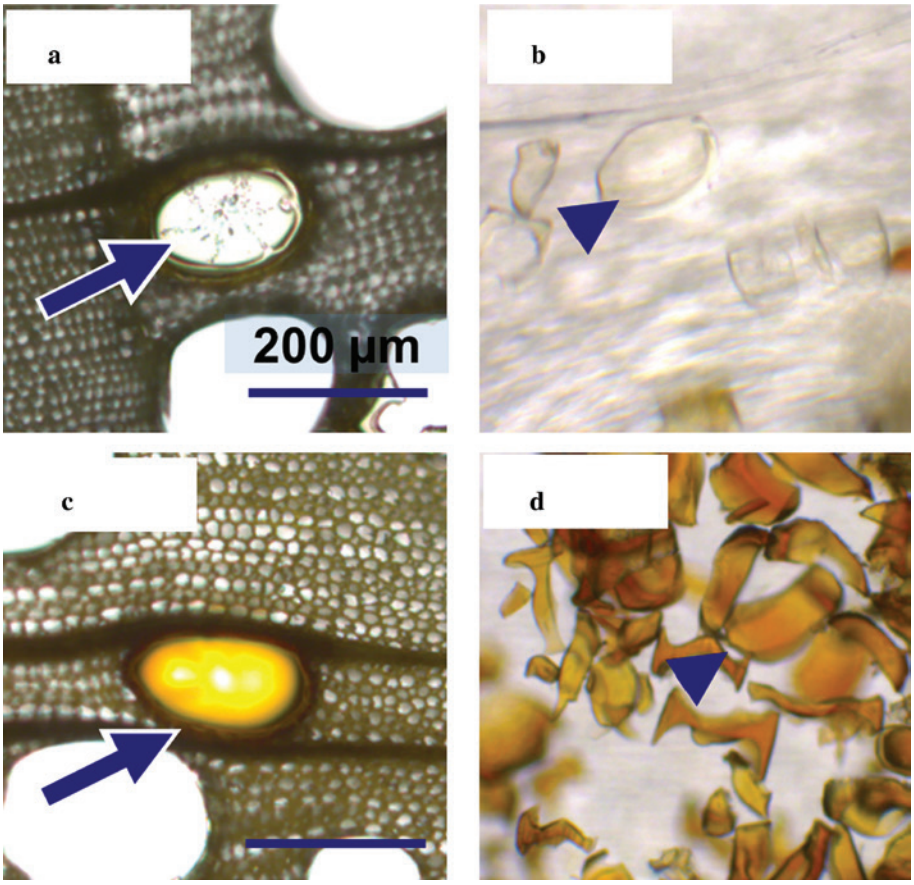

Figure 1: LMD collection of gum samples from the transverse sections of sW (a) and hW (c). Arrows indicate the gum positions in the sections. Arrowheads indicate the gums collected from sW (b) and hW (d).
Scale bars are 200 µm.

250°C; ion source 200°C. Six aromatic substances were identified by comparison with standard chemicals, which were purchased from Sigma-Aldrich Co. LLC. (St. Louis, MO, USA), Kanto Chemical Co., Inc. (Tokyo, Japan) and Tokyo Chemical Industry Co., Ltd. (Tokyo, Japan).

Results and discussion

Histochemical staining and UV microscopy

The results of the safranin-alcian blue staining of the *P. amurense* wood section with or without NaOH treatment are summarised in Figure 2. There were no gums in annual ring no. 1, neither in the intact nor in the NaOH-treated sections. Accordingly, the gums' synthesis began in annual ring no. 2. In the sW (annual rings nos. 2–4; Figure 2a–c) the double-stained gums with 1% safranin-alcian blue became blue, i.e. they reacted positively, which is typical to polysaccharides (Marjamaa et al. 2003; Graciano-Ribeiro and Nassar 2012). In the hW (annual rings nos. 5–9; Figure 2d–h), on the other hand, the gums turned red, which is indicative of aromatic substances (Marjamaa et al. 2003; Graciano-Ribeiro and Nassar 2012). Near the boundary of the sW and hW (annual ring no. 4, Figure 2c), some of the gums displayed a colour-changing trend from blue to red, which is a sign for the beginning of accumulation of aromatic substances.

In the NaOH-treated sections, the gums stained blue in the sW (Figure 2i and j), i.e. in the same way as in the intact sections. In the hW, the gums stained dark blue (Figure 2k–o). Notably, the inner edge of Figure 2m clearly exhibits a blue colour. This is a deviation from the behaviour of the intact sections and was interpreted as a part of the components in the hW gums becoming hydrolysed or extracted by the NaOH treatment, and thus probably having an aromatic character. Compared with the intact sections, there were no gums in annual ring no. 2 following the NaOH treatment (Figure 2), i.e. the gum disappeared, which might be the result of section shrinkage during the NaOH treatment. The staining results of the gums treated by HClaq, MeOH or DMSO were the same as in untreated

Brought to you by | Nagoya University
Authenticated
Download Date | 1/29/18 5:53 AM

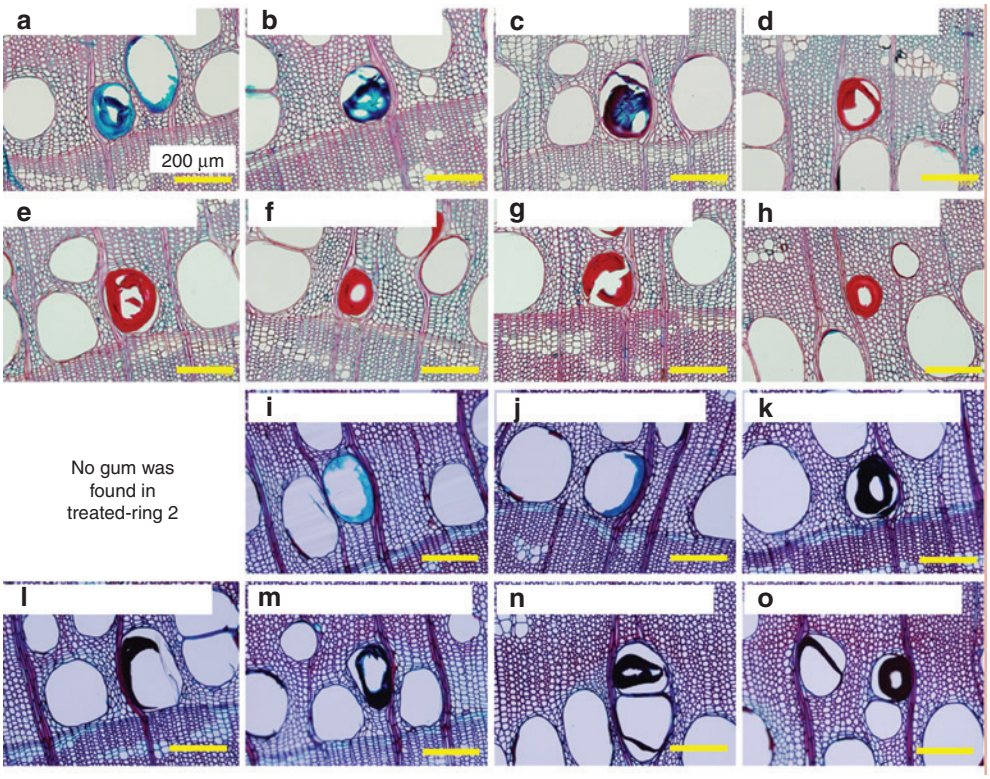

Figure 2: Typical images of intact (a–h) and NaOH-treated (i–o) gums from annual ring 2–9 double-stained with safranin-alcian blue. Scale bars are 200 µm.

tissues, i.e. blue in the sW and red in the hW (Figure S1). Accordingly, the gum components are insoluble in HClaq, MeOH or DMSO.

UV absorbance of hW gums was higher than that of sW gums (Figure 3), and this is indicative for the deposition of aromatic substances in the former. This finding is consistent with the results of the histochemical staining (Figure 2). That sW gum is made of polysaccharides and that hW gum has a pronounced aromatic character, which is consistent with findings of previous studies (Gagnon 1967; Rioux et al. 1998).

Raman microscopy

The Raman spectra of gums in sW and hW are presented in Figure 4. The bands at 1600 cm^{-1} and 1330 cm^{-1} are due to aromatic groups, while the bands at 1140 cm^{-1}, 1100 cm^{-1} and 880 cm^{-1} are originating from polysaccharides, and the band at 2940 cm^{-1} and the broad band around 3420 cm^{-1} are typical for C-H and O-H groups, respectively (Agarwal and Atalla 1986; Agarwal and Ralph 2008; Adar and Atalla 2010; Burikov et al. 2010; Ma et al. 2011; Ji et al. 2013).

In comparison with the band at 2940 cm^{-1}, the intensities of the bands at 1600 cm^{-1} and 1330 cm^{-1} are relatively higher in hW than in sW. Accordingly, the content of the aromatic substances in the former must be larger than that in the latter. This finding is consistent with both the histochemical staining and UV microscopy results (Figures 2 and 3). The bands at 1140, 1100, and 880 cm^{-1} in sW gums were significant, while those in hW gums were negligible, also in agreement with the findings stated above concerning the high polysaccharide content of the sW gums. Additionally, the O-H band around 3420 cm^{-1} decreased in the hW spectrum.

Previous studies (Ludwig 1952; Gagnon 1967; Aist 1983; Rioux et al. 1998) reported that pectin might constitute the basic component of gums, and other substances, such as phenolics that have also been detected either as part of these deposits or as accumulations alongside them. The detection of Raman bands with low intensity of polysaccharides in the hW gum is also indicative for their far higher aromatic content.

TOF-SIMS analysis

The sections containing sW and hW were measured by TOF-SIMS and the gum specific spectra were studied by

Brought to you by | Nagoya University
Authenticated
Download Date | 1/29/18 5:53 AM

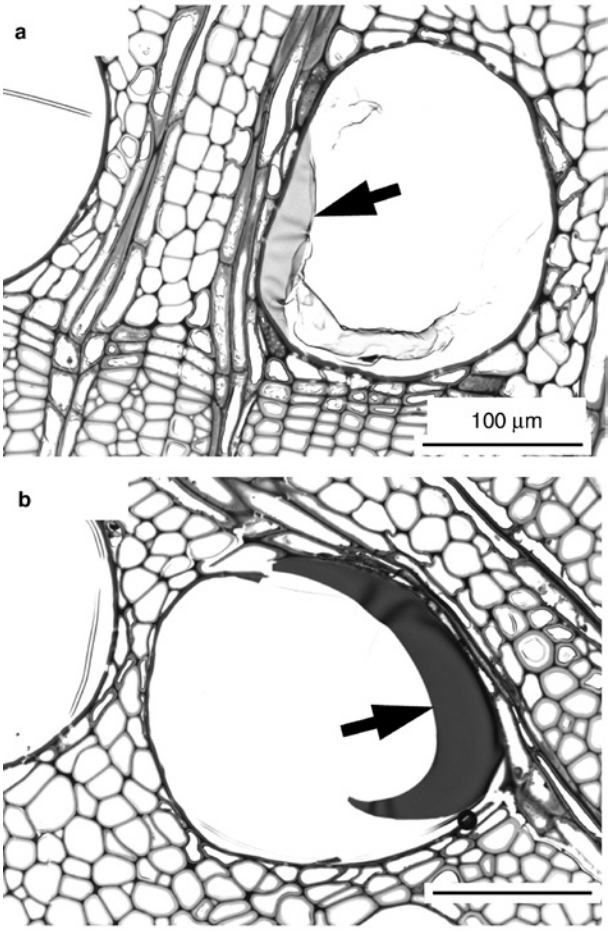

Figure 3: UV microscopic photographs of gums in (a) sW (annual ring 3) and (b) hW (annual ring 8).
The gums are indicated using arrows. Scale bars are 100 µm.

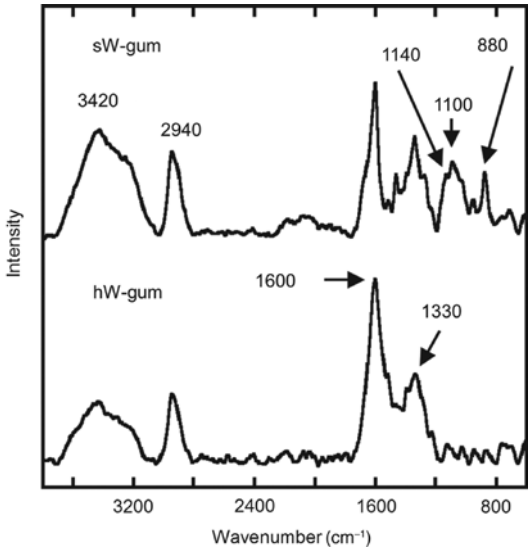

Figure 4: Raman spectra of gums in sW (annual ring 3) and hW (annual ring 8).

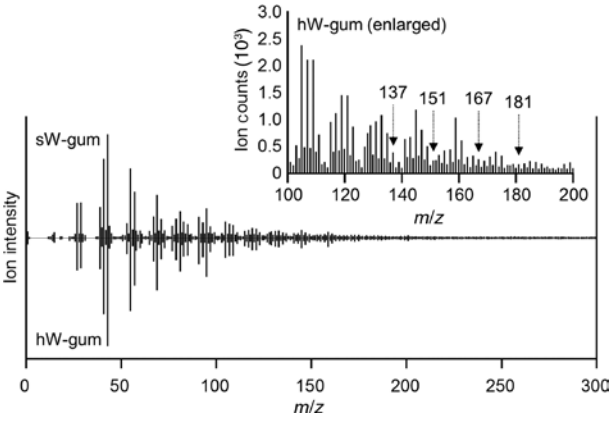

Figure 5: TOF-SIMS spectra of gums in sW and hW.
The enlarged scale of the hW gum spectrum was shown with the arrows indicating the position of *m*/*z* 137, 151, 167 and 181 ions.

ROI analysis. In Figure 5, the spectrum of sW-gum is displayed on the top and that of the hW-gum on the bottom. Unexpectedly, both gums exhibit nearly the same spectra with major secondary ions detectable below *m*/*z* 100.

In previous TOF-SIMS studies of plant cell walls, the secondary ions of *m*/*z* 137 and 151 are assigned to guaiacyl, and *m*/*z* 167 and 181 ions to syringyl lignin fragments, respectively (Saito et al. 2005; Goacher et al. 2011; Zheng et al. 2014a, 2016; Aoki et al. 2016a). In the present study, neither gum spectra showed significant ion peaks at these *m*/*z* values. Accordingly, there is no lignin in the gums. TOF-SIMS studies on hW in the literature report on the presence of low molecular weight compounds (Saito et al. 2008; Jyske et al. 2016; Mangindaan et al. 2017). In the present study, however, no secondary ions of low molecular weight substances are visible. This finding is interpreted that the aromatic substances deposited in the hW gums are not lignin; they are rather another type of cross-linked and condensed aromatic compounds.

Gums obtained by LMD and alkaline hydrolysis

The results of alkaline hydrolysis of the LMD isolated gums and intact wood sections are summarised in Table 1. Six aromatic compounds (vanillin, syringaldehyde, acetovanillone, acetosyringone, vanillic acid and syringic acid) were detected by GC-MS. As for the intact wood sections, vanillin, syringaldehyde, vanillic acid and syringic acid were detected under hydrolysis conditions with 1 M NaOHaq (60°C, 24 h). Following the 2 M NaOHaq (170°C, 2 h) treatment, the peak intensities of these compounds exhibit an increasing trend. Moreover, acetovanillone and

Brought to you by | Nagoya University
Authenticated
Download Date | 1/29/18 5:53 AM

Table 1: Aromatic compounds detected from intact wood sections and by LMD isolated gums via NaOHaq hydrolysis and subsequent GC-MS analysis.

	Intact wood sections				Gums collected by LMD			
	sW		hW		sW		hW	
Chemicals (area/mg-sample)	60°C	170°C	60°C	170°C	60°C	170°C	60°C	170°C
Vanillin	7.5E+06	6.8E+07	4.5E+06	9.9E+07	–	–	–	–
Syringaldehyde	4.3E+06	2.1E+08	3.3E+06	2.4E+08	–	–	–	–
Acetovanillone	–	5.5E+06	–	6.8E+06	–	–	–	–
Acetosyringone	–	2.6E+07	–	4.5E+07	–	–	–	–
Vanillic acid	1.4E+06	7.0E+06	1.1E+06	1.1E+07	–	–	3.8E+06	1.6E+07
Syringic acid	1.1E+06	3.8E+06	1.3E+06	1.7E+07	–	–	–	–

–, not detected. Values are the average of three samples.

acetosyringone additionally appeared following the 2 M NaOHaq treatment (Table 1).

As for gums collected by LMD, no aromatic compounds were detected in the sW material. Vanillic acid was detected in hW materials both after the 1 M and 2 M NaOHaq treatments (Table 1). As mentioned above, the isolated gums contain trace amounts of neighbouring cell wall materials (Figure 1). If the vanillic acid would be originating from the neighbouring cell wall of the gums, the other aromatic chemicals (vanillin, syringaldehyde, acetovanillone, acetosyringone, syringic acid) should also be detected. Therefore, it was concluded that the vanillic acid is derived from the aromatic deposits of the hW gums.

Vessel occlusion has an essential role in reducing the spread of pathogens after the vessels became dysfunctional by embolism (Zimmerman 1983; De Micco et al. 2016). It is possible that the secondary deposition of vanillic acid derivates makes the blockade by gum more effective, but it should be added in the same breath that nothing is known hitherto about this polymer, which has probably a polyester character.

Conclusion

The chemical composition and alteration of gums from sW to hW in *P. amurense* was investigated by means of microscopic and chemical methods. The results revealed that the framework of the gums in sW has the character of polysaccharides. Aromatic substances were accumulated in this substance during the conversion of the sW to hW. The entire structure of the aromatic substances remains unknown, but the presence of lignin may be probably excluded. The presence of vanillic acid in the alkaline hydrolysate in hW gum is indicative of a guaiacyl type aromatic polyester.

Acknowledgements: This work was supported by the JSPS KAKENHI Grant (25252032), China Postdoctoral Science Foundation (2015M582077) and Postdoctoral Innovation Project of Shandong Province (201503012). The authors thank Dr. Y. Nakata (Horiba Ltd.) for the Raman microscopy measurements and analyses.

References

Adar, F., Atalla, R. (2010) Analysis of lignin and cellulose in biological energy sources by Raman microscopy. Spectroscopy 25:18–23.

Agarwal, U.P., Atalla, R.H. (1986) In-situ Raman microprobe studies of plant cell walls: macromolecular organization and compositional variability in the secondary wall of *Picea mariana* (Mill.) BSP. Planta 169:325–332.

Agarwal, U.P., Ralph, S.A. (2008) Determination of ethylenic residues in wood and TMP of spruce by FT-Raman spectroscopy. Holzforschung 62:667–675.

Aist, J.R. (1983) Structural responses as resistance mechanisms. In: The Dynamics of Host Defence. Eds. Bailey, J.A., Deverall, B.J. Academic Press, Sydney. pp. 33–70.

Aoki, D., Saito, K., Matsushita, Y., Fukushima, K. (2016a) Distribution of cell wall components by TOF-SIMS. In: Secondary Xylem Biology. Eds. Kim, Y.S., Funada, R., Singh, A.P. Academic Press, London. pp. 363–377.

Aoki, D., Hanaya, Y., Akita, T., Matsushita, Y., Yoshida, M., Kuroda, K., Yagami, S., Takama, R., Fukushima, K. (2016b) Distribution of coniferin in freeze-fixed stem of *Ginkgo biloba* L. by cryo-TOF-SIMS/SEM. Sci. Rep. 6:31525.

Barnett, J.R., Cooper, P., Bonner, L.J. (1993) The protective layer as an extension of the apoplast. IAWA J. 14:163–171.

Bonsen, K.J.M., Kučera, L.J. (1990) Vessel occlusions in plants: morphological, functional and evolutionary aspects. IAWA J. 11:393–399.

Burikov, S., Dolenko, T., Patsaeva, S., Starokurov, Y., Yuzhakov, V. (2010) Raman and IR spectroscopy research on hydrogen bonding in water-ethanol systems. Mol. Phys. 108:2427–2436.

Chattaway, M.M. (1949) The development of tyloses and secretion of gum in heartwood formation. Aust. J. Biol. Sci. 2:227–240.

Brought to you by | Nagoya University
Authenticated
Download Date | 1/29/18 5:53 AM

De Micco, V., Balzano, A., Wheeler, E.A., Baas, P. (2016) Tyloses and gums: a review of structure, function and occurrence of vessel occlusions. IAWA J. 37:186–205.

Evert, R.F. Esau's Plant Anatomy: Meristems, Cells, and Tissues of the Plant Body – Their Structure, Function, and Development, 3rd ed. Wiley, Hoboken, 2006.

Fischer, S., Schenzel, K., Fischer, K., Diepenbrock, W. (2005) Applications of FT Raman spectroscopy and microspectroscopy characterizing cellulose and cellulosic biomaterials. Macromol. Symp. 223:41–56.

Foster, R.C. (1967) Fine structure of tyloses in three species of the Myrtaceae. Aust. J. Bot. 1:25–34.

Fujii, T., Lee, S.J., Kuroda, N., Suzuki, Y. (2001) Conductive function of intervessel pits through a growth ring boundary of *Machilus thunbergii*. IAWA J. 22:1–14.

Fujita, M., Shoji, Y., Harada, H. (1977) Vessel blockades by gum in *Albizia julibrissin* Durazz. and *Prunus jamasakura* Sieb. Bull. Kyoto Univ. For. 49:116–121 (in Japanese with English summary).

Gagnon, C. (1967) Histochemical studies on the alteration of lignin and pectic substances in white elm infected by *Ceratocystis ulmi*. Can. J. Bot. 45:1619–1623.

Gierlinger, N., Luss, S., König, C., Konnerth, J., Eder, M., Fratzl, P. (2010) Cellulose microfibril orientation of Picea abies and its variability at the micron-level determined by Raman imaging. J. Exp. Bot. 61:587–595.

Goacher, R.E., Jeremic, D., Master, E.R. (2011) Expanding the library of secondary ions that distinguish lignin and polysaccharides in time-of-flight secondary ion mass spectrometry analysis of wood. Anal. Chem. 83:804–812.

Graciano-Ribeiro, D., Nassar, N.M.A. (2012) A comparative anatomical study in cassava diploid and tetraploid hybrids. Plant Syst. Evol. 298:1711–1721.

Harem, M.K., Liman, N. (2009) Histochemical method for demonstrating quail mast cell types simultaneously. Biotech. Histochem. 84:275–282.

Hillis, W.E. Heartwood and tree exudates. Springer-Verlag, Berlin, 1987.

Ji, Z., Ma, J.F., Zhang, Z.H., Xu, F., Sun, R.C. (2013) Distribution of lignin and cellulose in compression wood tracheids of *Pinus yunnanensis* determined by fluorescence microscopy and confocal Raman microscopy. Ind Crops Prod. 47:212–217.

Jyske, T., Kuroda, K., Suuronen, J.P., Pranovich, A., Roig-Juan, S., Aoki, D., Fukushima, K. (2016) In planta localization of stilbenes within *Picea abies* phloem. Plant Physiol. 172:913–928.

Lee, Y.J., Perdian, D.C., Song, Z., Yeung, E.S., Nikolau, B.J. (2012) Use of mass spectrometry for imaging metabolites in plants. Plant J. 70:81–95.

Ludwig, R.A. (1952) Studies on the physiology of hadromycotic wilting in the tomato plant. Macdonald Coll. Tech. Bull. 20:1–40.

Ma, J., Zhang, Z., Yang, G., Mao, J., Xu, F. 2011. Ultrastructural topochemistry of cell wall polymers in *Populus nigra* by transmission electron microscopy and Raman imaging. Bioresources 6:3944–3959.

Mangindaan, B., Matsushita, Y., Aoki, D., Yagami, S., Kawamura, F., Fukushima, K. (2017) Analysis of distribution of wood extractives in *Gmelina arborea* by gas chromatography and time-of-flight secondary ion mass spectrometry. Holzforschung 71:299–305.

Marjamaa, K., Lehtonen, M., Lundell, T., Toikka, M., Saranpaa, P., Fagerstedt, K.V. (2003) Developmental lignification and seasonal variation in β–glucosidase and peroxidase activities in xylem of Scots pine, Norway spruce and silver birch. Tree Physiol. 23:977–986.

Meyer, R.W. (1967) Tyloses development in white oak. Forest Prod. J. 17:50–56.

Nakashima, J., Chen, F., Jackson, L., Shadle, G., Dixon, R.A. (2008) Multi-site genetic modification of monolignol biosynthesis in alfalfa (*Medicago sativa*): effects on lignin composition in specific cell types. New Phytol. 179:738–750.

Nakazono, M., Qiu, F., Borsuk, L.A., Schnable, P.S. (2003) Laser-capture microdissection, a tool for the global analysis of gene expression in specific plant cell types: identification of genes expressed differentially in epidermal cells or vascular tissues of maize. Plant Cell 15:583–596.

Nassar, N.M.A., Graciano-Ribeiro, D., Fernandes, S.D.C., Araujo, P.C. (2008) Anatomical alterations due to polyploidy in cassava, manihot esculenta crantz. Genet. Mol. Res. 7:276–283.

Pearce, R.B., Holloway, P.J. (1984) Suberin in the sapwood of oak (*Quercus robur* L.): its composition from a compartmentalization barrier and its occurrence in tyloses in undecayed wood. Physiol. Plant Pathol. 24:71–81.

Peetla, P., Schenzel, K.C., Diepenbrock, W. (2006) Determination of mechanical strength properties of hemp fibers using near-infrared fourier transform Raman microspectroscopy. Appl. Spectrosc. 60:682–691.

Rioux, D., Nicole, M., Simard, M., Ouellette, G.B. (1998) Immunocytochemical evidence that secretion of pectin occurs during gel (gum) and tylosis formation in trees. Phytopathol. 88:494–505.

Saito, K., Kato, T., Tsuji, Y., Fukushima, K. (2005) Identifying the characteristic secondary ions of lignin polymer using TOF-SIMS. Biomacromolecules, 6:678–683.

Saito, K., Mitsutani, T., Imai, T., Matsushita, Y., Fukushima, K. (2008) Discriminating the indistinguishable sapwood from heartwood in discolored ancient wood by direct molecular mapping of specific extractives using time-of-flight secondary ion mass spectrometry. Anal. Chem. 80:1552–1557.

Saitoh, T., Ohtani, J., Fukazawa, K. (1993) The occurrence and morphology of tyloses and gums in the vessels of Japanese hardwoods. IAWA J. 14:359–371.

Schenzel, K., Almlöf, H., Germgård, U. (2009) Quantitative analysis of the transformation process of cellulose I → cellulose II using NIR-FT Raman spectroscopy and chemometric methods. Cellulose 16:407–415.

Scott, J.E., Dorling, J. (1965) Differential staining of acid glycosaminoglycans (mucopolysaccharides) by alcian blue in salt solutions. Histochemie 5:221–233.

Wheeler, E.A. (2011) Inside wood – a web resource for hardwood anatomy. IAWA J. 32:199–211.

Zheng, P., Aoki, D., Yoshida, M., Matsushita, Y., Imai, T., Fukushima, K. (2014a) Lignification of ray parenchyma cells in xylem of *Pinus densiflora*. Part I: microscopic investigation by POM, UV microscopy, and TOF-SIMS. Holzforschung 68:897–905.

Zheng, P., Aoki, D., Matsushita, Y., Yagami, S., Fukushima, K. (2014b) Lignification of ray parenchyma cells in the xylem of *Pinus densiflora*. Part II: microchemical analysis by laser microdissection and thioacidolysis. Holzforschung 68:907–913.

Brought to you by | Nagoya University
Authenticated
Download Date | 1/29/18 5:53 AM

Zheng, P., Aoki, D., Matsushita, Y., Yagami, S., Sano, Y., Yoshida, M., Fukushima, K. (2016) Lignification of ray parenchyma cells (RPCs) in the xylem of *Phellodendron amurense* Rupr.: quantitative and structural investigation by TOF-SIMS and thioacidolysis of laser microdissection cuts of RPCs. Holzforschung 70:641–652.

Zheng, P., Ito, T., Aoki, D., Sato, S., Yoshida, M., Sano, Y., Matsushita, Y., Fukushima, K., Yoshida, K. (2017) Determination of inorganic element distribution in the freeze-fixed stem of $Al_2(SO_4)_3$-treated *Hydrangea macrophylla* by TOF-SIMS and ICP-AES. Holzforschung 71:471–480.

Zimmerman, M.H. Xylem structure and the ascent of sap. Springer-Verlag, New York, 1983.

Supplemental Material: The online version of this article offers supplementary material (https://doi.org/10.1515/hf-2017-0057).

Brought to you by | Nagoya University
Authenticated
Download Date | 1/29/18 5:53 AM